

# Diamonds and the African Lithosphere

F. R. BOYD AND JOHN J. GURNEY

Data and inferences drawn from studies of diamond inclusions, xenocrysts, and xenoliths in the kimberlites of southern Africa are combined to characterize the structure of that portion of the Kaapvaal craton that lies within the mantle. The craton has a root composed in large part of peridotites that are strongly depleted in basaltic components. The asthenosphere boundary shelves from depths of 170 to 190 kilometers beneath the craton to approximately 140 kilometers beneath the mobile belts bordering the craton on the south and west. The root formed earlier than 3 billion years ago, and at that time ambient temperatures in it were 900° to 1200°C; these temperatures are near those estimated from data for xenoliths erupted in the Late Cretaceous or from present-day heat-flow measurements. Many of the diamonds in southern Africa are believed to have crystallized in this root in Archean time and were xenocrysts in the kimberlites that brought them to the surface.

A LARGE FRACTION OF THE WORLD'S SUPPLY OF GEM AND industrial diamonds mined during the last century has come from the kimberlites and alluvial deposits of southern Africa. Obviously the diamonds have great economic importance. In addition, it now appears that the localization of diamond-bearing kimberlites within the Kaapvaal craton, together with data obtained from study of the minerals included in the diamonds and associated with them in rocks and concentrates, can be used to gain important insights into the structure and history of the craton.

High pressures are required for the crystallization of diamonds, corresponding to depths in the earth's mantle of at least 150 km, and diamonds formed at those depths have been brought to the surface in volcanic eruptions of kimberlite. They are found in minute concentrations (<1 part per million) in kimberlite that has filled the throats of ancient volcanoes, such as those at Kimberley, where igneous occurrences of diamonds were first recognized (1). Erosion of kimberlite pipes and transport of the diamonds in streams and rivers has dispersed them beyond the boundaries of the craton, in some cases forming secondary concentrations in stream gravels and beach deposits.

## Diamond Distribution

It has long been recognized that diamondiferous kimberlites are concentrated in the Kaapvaal craton (Fig. 1), the central part of southern Africa where the crustal basement is primarily composed of Archean gneisses, greenstones, and granitic rocks. Kimberlites occur widely throughout the southern part of the continent, but only those erupted within the boundaries of the craton contain significant quantities of diamonds.

Crustal rocks forming the surface of the craton are as old as  $3.5 \times 10^9$  years (2) and have formed a stable continental nucleus that has remained unaffected by orogeny for the past  $2.5 \times 10^9$  years (3). The Kaapvaal craton is surrounded on the south and west by belts of younger Precambrian rocks (Fig. 1). On the east it is rifted, and to the north it is joined to the craton in Zimbabwe by the Archean Limpopo belt.

That the pattern of occurrence of diamonds mirrors the surface exposure of the craton is extraordinary because it suggests that the conditions suitable for the formation of diamonds at depths of 150 km or more are linked with the occurrence of Archean rocks at the surface. Moreover, the physical connection appears to have been relatively rigid because eruption of diamonds in kimberlites within the craton has occurred over a period in excess of a billion years and because diamonds formed at depth have not been dispersed beyond craton boundaries by mantle flow. In other words, it appears that the craton may have a structure like that of an iceberg, with an ultramafic root in which diamonds have formed and a cap of ancient granitic gneisses and greenstones.

## Diamond Inclusions

Information about the composition and history of this root is being gathered through study of mineral inclusions in diamonds. These are usually monomineralic with a grain size of 10 to 100  $\mu\text{m}$ . Multiple, separate inclusions in individual diamonds are abundant, and there are tens of specimens from southern Africa that have been studied in which more than one mineral is included in a single diamond. Sulfides (pentlandite, pyrrhotite, and chalcopyrite) form the most abundant inclusions, but garnet, olivine, pyroxenes, and chromite are also relatively common. One major group of inclusions has minerals that commonly form olivine-bearing peridotites, whereas a second group has minerals that are characteristic of eclogites. These two parageneses never occur in a single diamond, but diamonds containing both occur together in some kimberlite pipes (4). The inclusions have been sealed from interaction with their surroundings from the time of their crystallization and incorporation in diamond.

The chemical isolation of these inclusions has made it possible to determine the age of crystallization of samples from three Kaapvaal localities. Welke and colleagues (5) made a pioneering determination by analyzing aggregate samples of sulfide inclusions extracted by ignition from diamonds from the Premier pipe. Isotopic ratios for trace amounts of lead in these inclusions were confirmed by Kramers (6) and are consistent with a model age near that of eruption of the Premier kimberlite [ $1.2 \times 10^9$  years (7)]. In addition, Kramers (6) analyzed sulfide inclusions from the Finsch and

F. R. Boyd is a petrologist at the Geophysical Laboratory, Carnegie Institution of Washington, 2801 Upton Street, NW, Washington, DC 20008. John J. Gurney is a geochemist in the Department of Geochemistry, University of Cape Town, Rondebosch, 7700, South Africa.

Kimberley pipes, obtaining model ages in excess of  $2 \times 10^9$  years. The ages of emplacement of the kimberlites at Finsch and Kimberley are about  $90 \times 10^6$  years (8), and the Precambrian model ages for diamonds from them are evidence that these diamonds were accidentally included in the kimberlite magmas. The Premier diamonds may also be xenocrysts, but this cannot be demonstrated on the basis of age relations.

It was impossible for Welke and colleagues or Kramers to distinguish between sulfide inclusions of peridotitic and eclogitic parageneses, although both may have been present in their samples and may have disparate ages. More exact ages for better-characterized samples were determined by Richardson and co-workers (9) for aggregates of separate garnet inclusions obtained by breaking numerous diamonds from the Finsch and Kimberley pipes. The garnet inclusions analyzed by these investigators were selected because they were rich in chromium, a characteristic of garnets in peridotitic mineral assemblages. Model neodymium-samarium ages of  $3.2 \times 10^9$  to  $3.3 \times 10^9$  years were obtained for duplicate samples for both localities, confirming and greatly refining Kramers' result. These age determinations reveal that the Kaapvaal root is ancient; the Archean crustal rocks are underlain at depths within the diamond stability field by mantle rocks of equivalent age.

The temperatures of crystallization of inclusion-bearing diamonds can be estimated from the partitioning of iron and magnesium between coexisting olivine and garnet or clinopyroxene and garnet (10, 11). Inasmuch as inclusions are usually separated in diamond, the iron-magnesium partitions reflect conditions at the time of crystallization rather than during any subsequent reequilibration (12). These temperature estimates are based on the assumption that the inclusions were in chemical equilibrium at the time of diamond formation. The assumption of equilibration is supported by the fact that multiple inclusions of a mineral in a single diamond commonly have the same composition (13). Partition thermometers have small pressure sensitivities, but the possible pressure range of equilibration for the inclusions is limited on the low side by the fact that crystallization has occurred within the diamond stability field.

Estimates for crystallization temperatures of inclusion pairs have the large range of  $900^\circ$  to  $1400^\circ\text{C}$  at an assumed pressure within the diamond field of 50 kbar (14). This range is four to five times  $2\sigma$  in application of the iron-magnesium partition thermometers (10). The solidus for ultramafic compositions in the presence of  $\text{H}_2\text{O}$  and  $\text{CO}_2$  has been estimated to be approximately  $1150^\circ\text{C}$  at 50 kbar [160 km (15)]. Crystallization temperatures of diamonds with eclogitic inclusions are uniformly above  $1100^\circ\text{C}$  at 50 kbar, whereas those of many with peridotitic inclusions are below  $1100^\circ\text{C}$  (12). That temperatures estimated for eclogite inclusions are predominantly restricted to the range above the volatile-present solidus is evidence that eclogitic diamonds may be igneous. Peridotitic diamonds with inclusions that have lower crystallization temperatures, on the other hand, may be of subsolidus origin, having formed in metamorphic or metasomatic events.

Formation of diamonds in either igneous or metasomatic events would have involved introduction of fluids from magmatic sources with temperatures at least as high as their overlying or surrounding rocks. The fluids can only have modified ambient temperatures by raising them. Thus, the lower temperatures estimated for diamond crystallization are those that most closely approximate ambient values. Pairs of olivine and garnet inclusions in diamonds from the Finsch kimberlite predominantly have crystallization temperatures in the range  $900^\circ$  to  $1100^\circ\text{C}$  at 50 kbar (12). These Finsch garnet-bearing diamonds form the largest suite of analyzed peridotitic inclusions, and their age of crystallization is near  $3 \times 10^9$  years (9). Estimates for 29 of these inclusion pairs, with allowance for the effects of pressure on the iron-magnesium partitions, overlap a

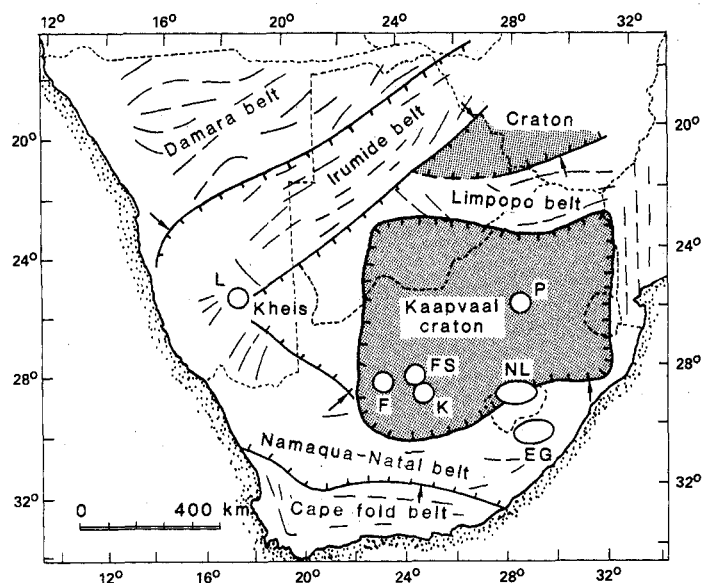


Fig. 1. Tectonic map of southern Africa [redrawn from (42)] showing the Archean cratons (shaded areas) and the surrounding mobile belts that are predominantly of Proterozoic age. Older provinces are on the ticked side of tectonic boundaries. Arrows indicate directions of overthrusting. The locations of kimberlite pipes or clusters of kimberlites mentioned in the text are indicated by circles and ellipses: L, Louwrensia; F, Finsch; FS, Frank Smith; K, Kimberley; P, Premier; NL, Northern Lesotho; and EG, East Griqualand.

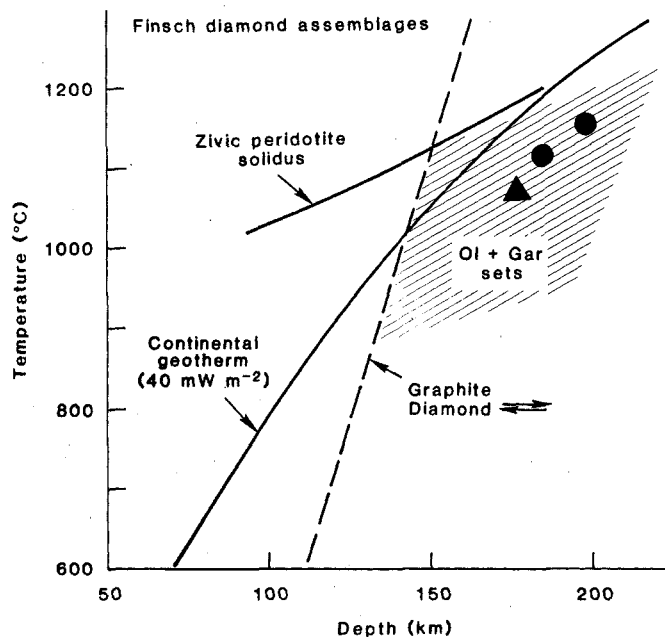
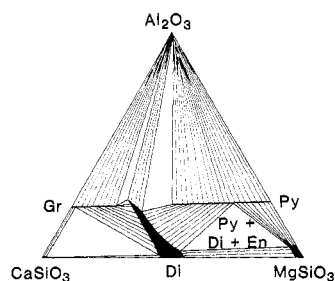


Fig. 2. Temperature-depth conditions of the origin of diamond inclusion sets and diamondiferous peridotite xenoliths from the Finsch kimberlite pipe, Kaapvaal craton [after (12)]. Also shown are a continental geotherm calculated for a heat flow of  $40 \text{ mW m}^{-2}$  (27), the diamond-graphite equilibrium boundary (43), and the solidus for peridotite in the presence of  $\text{CO}_2$  and  $\text{H}_2\text{O}$  [Zivc (15)]. The area defined by ruled lines is for the range of crystallization temperatures calculated by the method of O'Neill and Wood (10) for 29 sets of olivine plus garnet inclusions; the slope of the band is fixed by the pressure correction for this thermometer. Symbols: (▲) an assemblage of inclusions consisting of orthopyroxene plus olivine plus garnet in a single diamond (16); (●) diamondiferous lherzolite xenoliths (17). Equilibration conditions for the latter were calculated from the diopside solvus and the alumina content of enstatite (23). [Reprinted with permission from *Nature (London)*]

Fig. 3. Phase relations in the pure system  $\text{CaSiO}_3\text{-MgSiO}_3\text{-Al}_2\text{O}_3$  determined by analysis of coexisting phases in quenched charges equilibrated at 1200°C and 30 kbar [after (44)]. Symbols: Py, pyrope; Gr, grossularite; Di, diopside; En, enstatite. [Reprinted with permission from Mineralogical Society of America]



calculated continental geotherm based on an assumed heat flow of  $40 \text{ mW m}^{-2}$  (Fig. 2). One inclusion set from Finsch contains enstatite as well as olivine and garnet (16). A pressure of equilibration as well as a temperature can be estimated for this three-phase assemblage, and a pressure-temperature point for it plots within the diamond stability field close to the geotherm (Fig. 2).

Two garnet lherzolite xenoliths from the Finsch kimberlite contain diamonds (17). The minerals in these lherzolites were exposed to interaction with each other at high temperatures, possibly in the presence of pore fluids, until they were erupted in the Late Cretaceous (8). The equilibration of these rocks is thus markedly more recent than the temperatures of crystallization obtained for the Archean diamond inclusions. Nevertheless, the equilibration conditions for the diamond-bearing xenoliths also plot close to the geotherm (Fig. 2).

The data summarized in Fig. 2 suggest that temperatures in the root of the Kaapvaal craton in Archean time were near those calculated for a present-day shield geotherm. This conclusion is surprising in view of the fact that radioactive heat generation must have been considerably greater  $3 \times 10^9$  years ago than at present (18).

## Evidence from Concentrates

The largest fraction of crystalline mantle materials entrained in kimberlites is present as dispersed mineral grains rather than coherent xenoliths; in most kimberlites the proportion of grains to articulated xenoliths is greater than 100:1. The grains of disaggregated ultramafic rocks are concentrated in the course of prospecting or mining diamonds, and their study has provided evidence that some rocks forming the lithosphere at depth are only rarely erupted intact as xenoliths.

The compositions of most of the peridotitic garnets that form inclusions in diamonds are different from those of garnets in common peridotite xenoliths in that the diamond-inclusion garnets contain little calcium. Study of garnets from many kimberlite concentrates has shown that these unique, low-calcium garnets are present as coarse discrete grains wherever diamonds themselves are found (19). The coarse garnets are commonly 1 to 2 mm, in contrast to the inclusions that seldom exceed  $100 \mu\text{m}$ , and the low-calcium garnets are usually much more abundant in an individual kimberlite than are diamonds; hence, it seems unlikely that the discrete grains of low-calcium garnet originated as inclusions that were broken from diamonds. It is more likely that the coarse low-calcium garnets crystallized in rocks, probably in association with olivine, enstatite, chromite, and diamond.

The variations in calcium content in peridotite garnets reflect the different mineral assemblages in which they crystallized (20). Phase relations in the pure system  $\text{CaSiO}_3\text{-MgSiO}_3\text{-Al}_2\text{O}_3$  can be used to model the compositional variations of the natural garnets (Fig. 3). Olivine does not form solid solutions with pyroxene or garnet and

therefore need not be considered in this discussion. The three-phase field pyrope plus diopside plus enstatite (Fig. 3) represents the garnet lherzolite assemblage, and in the pure system the calcium content of the garnet is fixed at constant temperature and pressure. Garnets in natural peridotites contain additional elements and therefore have additional degrees of compositional freedom. Nevertheless, the calcium contents of natural peridotite garnets in equilibrium with diopside and enstatite are relatively constant and approximately equal to that shown for the three-phase field in Fig. 3. In the absence of diopside, however, garnet that is in equilibrium only with enstatite can have any calcium content less than the invariant composition, depending solely on the bulk composition of the assemblage. The two-phase field pyrope plus enstatite (Fig. 3) models natural garnet harzburgites, in which the garnets are poor in calcium.

Thus the coarse grains of low-calcium garnet that are abundant in some kimberlites are believed to have come from diopside-free garnet harzburgites despite the fact that only 10 to 20 specimens of such harzburgites have been found as articulated xenoliths in southern Africa. These harzburgites may have originated as residues from larger degrees of partial fusion and extraction of larger proportions of liquid than has commonly been the case in basalt formation. Possibly they are residues from the generation of komatiites (9, 21). The rare occurrence as xenoliths of the harzburgites with low-calcium garnets may have been caused by preferential disaggregation during eruption. It has been speculated that the disaggregation resulted from the hypothesized presence in them at depth of disseminated carbonate (magnesite) that underwent explosive decomposition and reaction during eruption (21, 22). If so, the carbonate and perhaps also the diamonds would appear to have been introduced in igneous or metasomatic events after the depletion. Richardson and colleagues (9) found that low-calcium garnets are enriched in neodymium and strontium relative to garnets from common peridotite xenoliths and suggested that the enrichment may have been caused by introduction of alkali- and light rare earth element-bearing melt before diamond crystallization.

Study of heavy-mineral concentrates from many kimberlites shows that there is a remarkable correlation between the occurrences

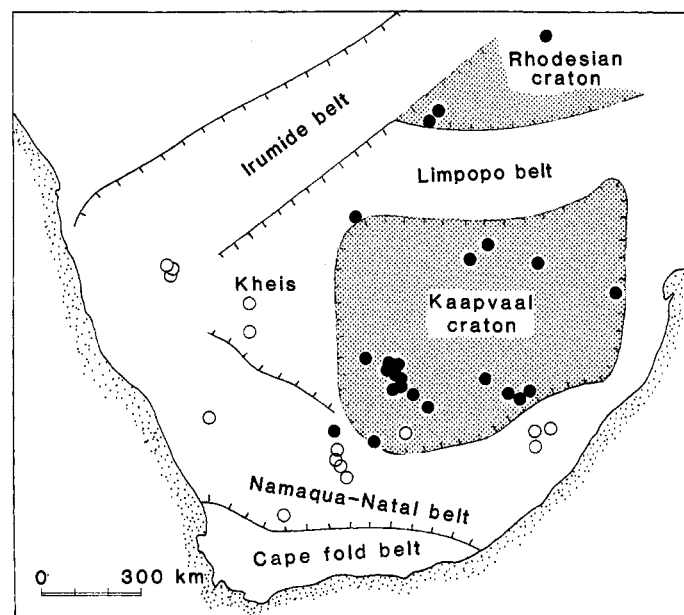


Fig. 4. Occurrences of low-calcium garnets in the kimberlites of southern Africa (●) and the locations of kimberlites where low-calcium garnets have been sought but not found (○) [data from (21, 45)]. Tectonic elements are from Fig. 1.

of these garnets and the tectonic setting of the kimberlite hosts (Fig. 4). All the kimberlites erupted within the craton boundaries that have been tested contain low-calcium garnets, whereas none have been found in kimberlites outside the craton and its margins. The distribution of low-calcium garnets thus matches the distribution of diamonds. Both appear to have originated as mineral grains in carbonate-bearing harzburgites that in southern Africa occur only in the root of the Kaapvaal craton.

## Mantle Xenoliths

The kimberlites of southern Africa contain a large number and variety of mantle xenoliths broken from conduit walls during eruption, although they are far less abundant than dispersed, individual grains. The mantle xenoliths are predominantly garnet peridotites, but eclogites, pyroxenites, dunites, and mica-rich and amphibole-rich xenoliths are present in some kimberlites and are locally abundant.

Most of the garnet-bearing xenoliths are of deep origin where ambient temperatures are above 800° to 900°C. The minerals in these rocks are usually homogeneous for major elements, and partitions of elements between minerals show systematic variations that are evidence of chemical equilibration (23). These partitions clearly reflect differences in temperature and depth of origin (24). Temperatures of equilibration for peridotite xenoliths can be estimated by application of a number of experimentally calibrated partition relations for calcium, magnesium, and iron that show rough agreement for most samples (23). There is currently only one well-calibrated barometer, the aluminum content of orthopyroxene in equilibrium with garnet (25, 26).

Temperature-depth estimates made for xenoliths from more than 20 kimberlite pipes in South Africa, Lesotho, and Southwest Africa–Namibia form two groups. Temperature-depth estimates for low-temperature xenoliths from southern Africa all plot close to a geotherm calculated for a continental shield with a heat flow of 40 mW m<sup>-2</sup> (27). Estimates for high-temperature xenoliths, however, deviate from the geotherm toward higher temperatures. The patterns of points for temperature-depth estimates calculated for individual xenolith suites (Fig. 5) appear to form perturbed geotherms (24). The points for high-temperature xenoliths that deviate from normal geotherms have been interpreted to represent thermal anomalies caused by convective movements in the asthenosphere, possibly diapiric (28), with eruptions originating at the base of the lithosphere (29, 30). An alternative view is that the high-temperature xenoliths formed in contact aureoles enveloping magma chambers within the lithosphere having dimensions that were more restricted than expected for diapirs (31). The former interpretation, however, provides an explanation for the regular variations in the depths of origin of the high-temperature peridotites (Fig. 5).

The depth of origin of the high-temperature xenoliths is systematically greater for those erupted within the boundaries of the Kaapvaal craton than for those erupted in areas peripheral to the craton. These regularities are evidence that a plane in the mantle beneath southern Africa defined by the transition between low- and high-temperature peridotites represents a boundary in physical and perhaps chemical properties. This plane is approximately isothermal, having a temperature of 1000° to 1150°C. The solidus for peridotite in the presence of small amounts of H<sub>2</sub>O and CO<sub>2</sub> is about 1150°C at 50 kbar (15). Thus the transition between the low- and high-temperature peridotites is in approximate concordance with the expected beginning of melting in the presence of volatiles. The high-temperature peridotites were not melted at the time of eruption because they were dry, but evidence for the existence of liquid in

their depth range is provided by megacrysts, many of which are believed to have been crystals in liquid at the time of eruption (32, 33). It is reasonable to suppose that the xenolith transition marks the beginning of melting where volatiles were present and was an asthenosphere-lithosphere boundary at the time of kimberlite eruption. The evidence provided by the xenolith and megacryst suites is interpreted as indicating that the distribution of volatiles and accompanied melting was irregular.

The depth to the transition is 170 to 190 km within the boundaries of the craton but decreases to 140 km in the Gibeon area west of the craton in Southwest Africa–Namibia and in the East Griqualand area southeast of the craton. These regularities in the depths of the transition are interpreted as delineating a root for the Kaapvaal craton. A cross section of the lithosphere beneath southern Africa extending from Gibeon at the northwest across the craton to East Griqualand on the southeast shows the proposed root in relation to the diamond-graphite equilibrium boundary (Fig. 6). The lithosphere extends into the diamond stability field only in the root. The temperature-depth relations for xenoliths can thus be used to quantify the hypothesis of a Kaapvaal root, developed in combination with evidence obtained from the study of diamond inclusions and garnet xenocrysts.

## Discussion

The relief on the lithosphere-asthenosphere boundary beneath southern Africa appears to have been about 40 km at the time of kimberlite eruption 90 × 10<sup>6</sup> years ago, shelving from a depth of 170 to 190 km beneath the craton to 140 km beneath the mobile belts. Further thinning must have occurred in the transition from the mobile belts to the Atlantic and Indian Ocean basins. Isotopic investigations of inclusions in diamonds have provided evidence that

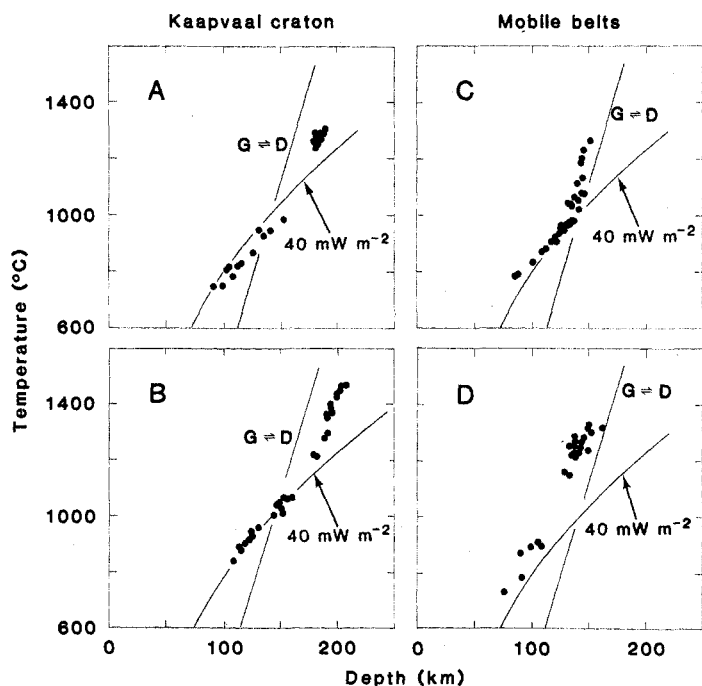


Fig. 5. Temperature-depth conditions of equilibration of four suites of xenoliths from southern Africa calculated by pyroxene thermobarometry (23). The Frank Smith (A) and northern Lesotho (B) suites are from the craton, whereas Louwrencia (C) is west of the craton and East Griqualand (D) is to the southeast (Fig. 1). The diamond-graphite equilibrium boundary ( $G=D$ ) (43) and a continental geotherm (27) are included for reference.

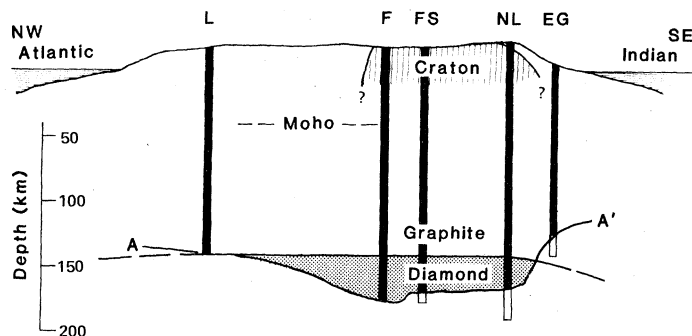


Fig. 6. Model for the lithosphere beneath southern Africa based on geothermobarometry for xenolith suites. Ratio of depth scale to horizontal scale is 4:1 below sea level; the topography shown is greatly exaggerated. Vertical bars represent xenolith suites, and the maximum depths shown are for clusters of xenoliths of deepest origin in each suite. The line A-A' is approximately the locus of points of inflection in the xenolith geotherms, or the breaks between clusters of points for high- and low-temperature xenoliths (Fig. 5). The xenolith suites are L, Louwrensia; F, Finsch; FS, Frank Smith; NL, northern Lesotho; and EG, East Griqualand. The graphite-diamond transition is represented by a line drawn through the points of intersection of individual xenolith geotherms with the equilibrium boundary of Kennedy and Kennedy (43).

the Kaapvaal root is more than  $3 \times 10^9$  years in age, and applications of element-partition geothermometry and barometry indicate that temperatures in the root in Archean time were relatively cool ( $900^\circ$  to  $1200^\circ\text{C}$ ), similar to those estimated from present-day heat flow (27). These results provide a useful framework for further speculation about the early history of the craton and the earth as a whole, but they leave many questions unanswered.

Peridotites making up the craton have substantially higher ratios of magnesium to magnesium plus iron [ $\text{Mg}/(\text{Mg} + \text{Fe})$ ] in their mineral (for example, olivine) and whole-rock compositions than do peridotites that have formed in oceanic lithosphere. Olivines in low-temperature peridotites from the craton have  $\text{Mg}/(\text{Mg} + \text{Fe})$  ratios that are predominantly 0.92 to 0.93 (34, 35), whereas those from ophiolite tectonites (36) and abyssal peridotites (37) have predominant values of 0.91. Jordan (38) has suggested that this compositional difference has stabilized a thermal gradient between the upper mantle beneath the ocean basins and relatively cooler mantle beneath the continents. The difference is small, but it reflects an important difference in the igneous processes by which the two kinds of lithosphere have formed. Continental cratons may be composed of more magnesium-rich residues from greater degrees of partial melting during Archean magma generation than have occurred in the more recent formation of oceanic lithosphere. Whether garnet peridotite xenoliths that have been erupted from beneath the mobile belts have significant differences in the range of  $\text{Mg}/(\text{Mg} + \text{Fe})$  values from those of craton origin is not yet clear.

Dike and vein structures that involve lithologic contrasts have been found in many ultramafic xenoliths erupted in alkali basalts (39). Xenoliths with similar structures have been found in kimberlites (40, 41), but they are extremely rare in proportion to those peridotites that are texturally and compositionally homogeneous. An impression gained from study of the common peridotites is that the igneous events in which cratons were constructed left residues of remarkable uniformity. Differences in basaltic and kimberlithic xenolith suites are obviously related in part to depth of origin. The garnet-bearing peridotites in kimberlites have come from greater depths than the spinel-bearing peridotites in basalts. The compositional and structural differences may also, however, reflect differences in tectonic environment. The lithosphere from which basalt xenoliths have been derived appears to be more like that formed beneath ocean basins than that within continental cratons.

The localization of free carbon as diamond or graphite within the craton is not yet fully understood. The results discussed above provide evidence that diamond is stable in lithosphere rocks only beneath the craton and that beneath the mobile belts the lithosphere is predominantly or entirely within the graphite stability field. The abundance of graphite is comparable to that of diamond in eclogites and peridotites that have been erupted within the craton, and the two occur together in rare xenoliths (4). Pyroxene thermobarometry provides evidence that most graphite-bearing peridotites have formed at shallower depths than those containing diamond (14), but graphite has not yet been found in peridotite or eclogite xenoliths erupted from the mantle beneath the mobile belts. Thus it may not be sufficient to explain the stable occurrence of diamond within the craton. The unknown processes by which carbon is precipitated in the mantle in elemental form may also be localized within the craton.

The concentration of low-calcium garnets within the craton and their association with diamonds, both as inclusions and as coexisting xenocrysts in kimberlite, remains a puzzle. Diamonds occur in eclogites and in rare lherzolites as well as in association with low-calcium garnets. Thus there may be no genetic basis for the association between the garnets and diamonds. The root of the Kaapvaal craton is believed to contain large amounts of strongly depleted, low-calcium garnet harzburgites, but it is possible that these are common hosts to diamonds only because of their tectonic position. Why then are these strongly depleted harzburgites present only within the craton and never in the lithosphere beneath the mobile belts? The answer to this question may link the occurrence of the harzburgites with that of Archean komatiites and with a Proterozoic age for the formation of the lithosphere beneath the mobile belts.

#### REFERENCES AND NOTES

1. J. B. Dawson, *Kimberlites and Their Xenoliths* (Springer-Verlag, Berlin, 1980).
2. P. J. Hamilton, N. M. Evenson, R. K. O'Nions, H. S. Smith, A. J. Erlank, *Nature (London)* **279**, 298 (1979).
3. M. J. Viljoen and R. P. Viljoen, in *African Magmatism and Tectonics*, T. N. Clifford and I. G. Gass, Eds. (Hafner, Darien, CT, 1970), pp. 27-49.
4. J. J. Gurney, J. W. Harris, R. S. Rickard, in *Kimberlites II: The Mantle and Crust-Mantle Relationships*, J. Kornprobst, Ed. (Elsevier, Amsterdam, 1984), pp. 25-32.
5. H. J. Welke, H. L. Allsopp, J. W. Harris, *Nature (London)* **252**, 35 (1974).
6. J. D. Kramers, *Earth Planet. Sci. Lett.* **42**, 58 (1979).
7. D. R. Barrett and H. L. Allsopp, *Extended Abstracts, First International Kimberlite Conference*, Cape Town, South Africa, September 1973, pp. 23-25.
8. G. L. Davis, *Extended Abstract, Second International Kimberlite Conference*, Sante Fe, NM, 3 to 7 October 1977.
9. S. H. Richardson, J. J. Gurney, A. J. Erlank, J. W. Harris, *Nature (London)* **310**, 198 (1984).
10. H. St. C. O'Neill and B. J. Wood, *Contrib. Mineral. Petrol.* **70**, 59 (1979).
11. D. J. Ellis and D. H. Green, *ibid.* **71**, 13 (1979).
12. F. R. Boyd, J. J. Gurney, S. H. Richardson, *Nature (London)* **315**, 387 (1985).
13. J. J. Gurney, J. W. Harris, R. S. Rickard, in *Proceedings of the 2nd International Kimberlite Conference*, F. R. Boyd and H. O. A. Meyer, Eds. (American Geophysical Union, Washington, DC, 1979), vol. 1, pp. 1-15.
14. F. R. Boyd and A. A. Finnerty, *J. Geophys. Res.* **85**, 6911 (1980).
15. D. H. Eggler and R. F. Wendlandt, in *Proceedings of the 2nd International Kimberlite Conference*, F. R. Boyd and H. O. A. Meyer, Eds. (American Geophysical Union, Washington, DC, 1979), vol. 1, pp. 330-338.
16. H.-M. Tsai, H. O. A. Meyer, J. Moreau, H. J. Milledge, *ibid.*, pp. 16-26.
17. S. R. Shee, J. J. Gurney, D. N. Robinson, *Contrib. Mineral. Petrol.* **81**, 79 (1982).
18. W. R. Dickinson and W. C. Luth, *Science* **174**, 400 (1971).
19. J. J. Gurney and G. S. Switzer, *Contrib. Mineral. Petrol.* **39**, 103 (1973).
20. N. V. Sobolev, Yu. G. Lavrent'ev, N. P. Pokhilenko, L. V. Usova, *ibid.* **40**, 39 (1973).
21. F. R. Boyd and J. J. Gurney, *Carnegie Inst. Washington Yearb.* **81**, 261 (1982).
22. P. J. Wyllie, W. L. Huang, J. Otto, A. P. Byrnes, *Tectonophysics* **100**, 359 (1983).
23. A. A. Finnerty and F. R. Boyd, *Geochim. Cosmochim. Acta* **48**, 15 (1984).
24. F. R. Boyd, *ibid.* **37**, 2533 (1973).
25. I. D. MacGregor, *Am. Mineral.* **59**, 110 (1974).
26. D. Perkins, III, T. J. B. Holland, R. C. Newton, *Contrib. Mineral. Petrol.* **78**, 99 (1981).
27. H. N. Pollack and D. S. Chapman, *Tectonophysics* **38**, 279 (1977).
28. H. W. Green and Y. Gueguen, *Nature (London)* **249**, 617 (1974).
29. F. R. Boyd, *Carnegie Inst. Washington Yearb.* **75**, 521 (1976).
30. ——— and P. H. Nixon, *Geochim. Cosmochim. Acta* **42**, 1367 (1978).
31. B. Harte, in *Continental Basalts and Mantle Xenoliths*, C. J. Hawkesworth and M. J. Norry, Eds. (Shiva, Cheshire, U.K. 1983).

32. P. H. Nixon and F. R. Boyd, in *Lesotho Kimberlites*, P. H. Nixon, Ed. (Lesotho National Development Corporation, Maseru, Lesotho, 1973), pp. 67-75.
33. J. J. Gurney, W. R. O. Jakob, J. B. Dawson, in *Proceedings of the 2nd International Kimberlite Conference*, F. R. Boyd and H. O. A. Meyer, Eds. (American Geophysical Union, Washington, DC, 1979), vol. 2, pp. 227-243.
34. R. V. Danchin and F. R. Boyd, *Carnegie Inst. Washington Yearb.* 75, 531 (1976).
35. M. J. O'Hara, M. J. Saunders, E. L. P. Mercy, *Phys. Chem. Earth* 9, 571 (1975).
36. R. G. Coleman, *Ophiolites* (Springer-Verlag, Berlin, 1977).
37. H. J. B. Dick and R. L. Fisher, in *Kimberlites II: The Mantle and Crust-Mantle Relationships*, J. Kornprobst, Ed. (Elsevier, Amsterdam, 1984), pp. 295-308.
38. T. H. Jordan, in *Proceedings of the 2nd International Kimberlite Conference*, F. R. Boyd and H. O. A. Meyer, Eds. (American Geophysical Union, Washington, DC, 1979), vol. 2, pp. 1-14.
39. H. G. Wilshire *et al.*, *U.S. Geol. Surv. Open-File Rep.* 85-139 (1985).
40. K. G. Cox, J. J. Gurney, B. Harte, in *Lesotho Kimberlites*, P. H. Nixon, Ed. (Lesotho National Development Corporation, Maseru, Lesotho, 1973), pp. 76-98.
41. A. P. Jones, J. V. Smith, J. B. Dawson, *J. Geol.* 90, 435 (1982).
42. P. H. Nixon, F. R. Boyd, N. Z. Boctor, *Trans. Geol. Soc. S. Afr.* 86, 221 (1983).
43. C. S. Kennedy and G. C. Kennedy, *J. Geophys. Res.* 81, 2467 (1976).
44. F. R. Boyd, *Mineral. Soc. Am. Spec. Pap.* 3, 63 (1970).
45. J. J. Gurney, unpublished data.
46. We have benefited from helpful remarks on this manuscript by P. H. Nixon and H. S. Yoder, Jr. We thank J. B. Hawthorne for his assistance in arranging field studies. J.J.G. acknowledges financial support for research from DeBeers Consolidated Mines, Ltd. Research by F.R.B. was supported under NSF grants EAR-7924567, 8120832, 8418447, and 8417437.

## Research Articles

# Biochemical and Genetic Evidence for the Hepatitis B Virus Replication Strategy

CHRISTOPH SEEGER, DON GANEM, HAROLD E. VARMUS

Hepatitis B viruses synthesize their open circular DNA genomes by reverse transcription of an RNA intermediate. The details of this process have been examined with the use of mammalian hepatitis B viruses to map the sites for initiation and termination of DNA synthesis and to explore the consequences of mutations introduced at short, separated direct repeats (DR1 and DR2) implicated in the mechanisms of initiation. The first DNA strand to be synthesized is initiated within DR1, apparently by a protein primer, and the completed strand has a short terminal redundancy. In contrast, the second DNA strand begins with the sequence adjacent to DR2, but its 5' end is joined to an oligoribonucleotide that contains DR1; thus the putative RNA primer has been transposed to the position of DR2. It is now possible to propose a detailed strategy for reverse transcription by hepatitis B viruses that can be instructively compared with that used by retroviruses.

RNA-DIRECTED DNA SYNTHESIS, FIRST DESCRIBED FOR retroviruses (1, 2), is now recognized as the probable means for transfer of genetic information in various other settings, such as the replication of hepatitis B (3) and cauliflower mosaic viruses (4); the transposition of some eukaryotic mobile elements, including the yeast Ty elements (5-7) and the  *copia* -like elements of  *Drosophila*  (8); and the generation of several repeated components of eukaryotic genomes, including processed pseudogenes (9, 10), some repeated dispersed sequences (11), and possibly the abundant Alu-like repeats (10).

The synthesis of double-stranded DNA from a single-stranded RNA template requires (i) an enzyme for synthesizing the first DNA strand from an RNA template and the second DNA strand from the first; (ii) primers for each of the two strands; and (iii) a means for removing the RNA template after reverse transcription, to allow synthesis of the second DNA strand. In some cases, strategies for duplicating sequences are required. For example,

retrotransposons must not only perpetuate all of the single copy sequences present in the RNA template, but also generate two copies of sequences present once in the RNA to form long terminal repeats (LTR's) in DNA (2, 5, 12).

For retroviruses, the cardinal features of reverse transcription have been elucidated: (i) the first strand is primed by a host transfer RNA (tRNA) base-paired to the viral RNA genome near its 5' end; (ii) the second strand is primed by a viral RNA oligomer that is produced from a polypurine region by a ribonuclease (RNase) activity associated with reverse transcriptase and specific for RNA-DNA hybrids (RNase H); (iii) a terminal redundancy (R) in viral RNA and complementarity between the ends of nascent strands facilitate transfer of nascent strands twice between templates, without loss of genetic material; and (iv) the finished product, a linear DNA duplex, displays LTR's composed mainly of sequences present only once in viral RNA (2). Structural analyses of transposable elements of yeast and  *Drosophila*  suggest that their replication strategies are likely to be fundamentally similar to those used by retroviruses (5, 6, 13).

The hepatitis B viruses (hepadnaviruses) differ fundamentally from retroviruses in that the form of the genome present in mature virus particles is DNA rather than RNA. These strongly hepatotropic agents have now been isolated from man, woodchucks, ground squirrels, and ducks, and they are important causes of liver disease in man and woodchucks (14). The discovery by Summers and Mason and colleagues that hepadnaviruses replicate by reverse transcription of RNA intermediates was based on the analysis of virus-specific nucleic acids and subviral particles from infected duck livers (3, 15). In contrast to the products of semiconservative DNA replication, hepatitis B virus DNA is asymmetric, with the strand complementary to viral RNA (the minus strand) longer and more abundant than the plus strand (15, 16). Isolated particles synthesize minus strand DNA in the presence of actinomycin D, and the product of

C. Seeger is a postdoctoral fellow in the Department of Microbiology and Immunology, D. Ganem is an assistant professor in the Departments of Medicine and Microbiology and Immunology, and H. E. Varmus is a professor in the Departments of Microbiology and Immunology and Biochemistry and Biophysics, University of California, San Francisco, CA 94143.